

# Analytical theory of frequency-multiplying gyro-traveling-wave-tubes

G. S. Nusinovich,<sup>a)</sup> W. Chen, and V. L. Granatstein

*Institute for Plasma Research, University of Maryland, College Park, Maryland 20742*

(Received 10 August 2000; accepted 1 November 2000)

The theory is developed which describes analytically the gain and bandwidth in frequency-multiplying gyro-traveling-wave-tubes. In this theory the input waveguide is considered in the small-signal approximation. Then, in the drift region separating the input and output waveguides, the electron ballistic bunching evolves which causes the appearance in the electron current density of the harmonics of the signal frequency. The excitation of the output waveguide by one of these harmonics is considered in a specified current approximation. This makes the analytical study of a large-signal operation possible. The theory is illustrated by using it to analyze the performance of an existing experimental tube. © 2001 American Institute of Physics.

[DOI: 10.1063/1.1335830]

## I. INTRODUCTION

There is considerable interest in the development of compact, high-power, millimeter-wave amplifiers for advanced radar applications. As is known (see, e.g., Ref. 1), among such amplifiers the devices capable of delivering the highest average power are gyroamplifiers. However, their use in radar can be restricted by magnetic fields required for generating electromagnetic waves with frequencies close to the cyclotron frequency of gyrating electrons. To alleviate the magnetic field requirement, one can develop gyroamplifiers operating at harmonics of the cyclotron frequency (see, e.g., Ref. 2 for second harmonic gyroklystrons and Ref. 3 for second-harmonic gyro-traveling-wave-tubes).

When such devices consist of several stages it is beneficial in some cases to operate in frequency-multiplying regimes. In these regimes the benefits from operation at cyclotron harmonics can be combined with the advantages of using available, relatively inexpensive, low-frequency, high-power drivers for input stages of such amplifiers. In recent years such frequency-multiplying operation of various gyroamplifiers was studied at the University of Maryland both experimentally<sup>4-6</sup> and theoretically.<sup>7-11</sup>

One of the most promising large-bandwidth gyroamplifiers is the gyro-traveling-wave-tube (gyro-TWT). These tubes have been under development at the Naval Research Laboratory (NRL) for a long time: in the late 1970s the first proof-of-principle experiments were carried out<sup>12</sup> in which the bandwidth was only about 1.4%. Very soon, in the early 1980s, the use of the properly tapered waveguide and external magnetic field allowed NRL researchers to enlarge the bandwidth up to 13%.<sup>13</sup> Later, in a tapered two-stage configuration the 20% bandwidth was demonstrated.<sup>14</sup> (The theory of such tapered two-stage gyro-TWTs is developed in Refs. 15 and 16.) Another group where gyro-TWTs are being actively developed is the National Tsing Hua University, Taiwan. Recently, the efforts of this group culminated in the development of a 100 kW level, Ka-band gyro-TWT with a

3% bandwidth and 70 dB gain.<sup>17</sup> The success of this group initiated an interest in their concept at NRL.<sup>18</sup>

In regard to the frequency-multiplying multistage gyro-TWTs, let us point out that, although some important theoretical issues were outlined in Ref. 11 where some results of simulations for two-stage, frequency-doubling devices were presented, the analytical theory for such devices is not yet developed. In the present study we make an attempt to develop a simple version of such a theory which allows one to analyze the gain, bandwidth, and saturation effects in frequency-multiplying gyro-TWTs. Our theory is based on the formalism used in Ref. 19 for developing the linear theory of multistage gyro-TWTs. At this point we should remind our readers that the frequency multiplication is a purely nonlinear process, which occurs in an initially modulated electron beam due to its nonlinear properties. These nonlinear properties can be associated with the electron ballistic bunching evolving in the drift region between the input and output stages.<sup>20</sup> Correspondingly, the input waveguide can be considered in the frame of the linear theory. Then, the appearance of signal frequency harmonics in the electron current density can easily be analyzed in the drift region which is free of electromagnetic waves. Finally, the excitation of a relatively short output waveguide by a prebunched beam can be studied in a specified current approximation, which greatly simplifies the nonlinear analysis of the device. The last approximation was also adopted in Refs. 15 and 16 (see also Refs. 19 and 21).

Our article is organized as follows. Section II contains a general formalism. In Sec. III we present the results. In Sec. IV we discuss an applicability of our formalism and results to the analysis and design of real devices. In Sec. V we summarize our study. In the Appendix we compare the results of the analysis of the output waveguide operation with and without the use of a specified current approximation.

## II. GENERAL FORMALISM

Below we will consider a two-stage gyro-TWT assuming that we can neglect the space charge effects and the

<sup>a)</sup>Electronic mail: gregoryn@Glue.umd.edu

electron spread in velocities and guiding center radii, as well as the interaction of electrons with the nonsynchronous backward wave. (Recall that the latter implies the waveguide operation far from cutoff.) Then, as discussed in detail elsewhere,<sup>22,23</sup> the operation of the gyro-TWT can be described by equations for the slowly variable normalized electron energy  $w$ , phase  $\theta$ , and wave amplitude  $F$ :

$$\frac{dw}{d\zeta} = -2 \frac{(1-w)^{s/2}}{1-bw} \operatorname{Re}(F e^{-is\theta}), \quad (1)$$

$$\frac{d\theta}{d\zeta} = \frac{1}{1-bw} \{w - \Delta + (1-w)^{s/2-1} \operatorname{Im}(F e^{-is\theta})\}, \quad (2)$$

$$\frac{dF}{d\zeta} = -I_0 \frac{1}{2\pi} \int_0^{2\pi} \frac{(1-w)^{s/2}}{1-bw} e^{is\theta} d\theta_0. \quad (3)$$

Here  $w = 2[(1 - h\beta_{z0})/\beta_{\perp 0}^2][\gamma_0 - \gamma]/\gamma_0$  is the normalized variable describing the changes in electron energy,  $h = k_z c/\omega$  is the normalized axial wave number,  $\beta_{z0}$  and  $\beta_{\perp 0}$  are, respectively, the initial axial and orbital electron velocities normalized to the speed of light,  $\gamma$  is the electron energy normalized to the rest energy, and  $\gamma_0$  is its value at the entrance. Also in Eqs. (1)–(3),  $\zeta = [\beta_{\perp 0}^2(1 - h^2)/2\beta_{z0}(1 - h\beta_{z0})](\omega z/sc)$  is the normalized axial coordinate, and parameter  $b = h\beta_{\perp 0}^2/2\beta_{z0}(1 - h\beta_{z0})$  characterizes the changes in the electron axial velocity with the change in electron energy in the process of interaction with the wave. The phase  $\theta = \Theta - (\omega t - k_z z + \psi)/s$  is the slowly variable gyrophase of electrons with respect to the phase of the wave,  $s$  is the cyclotron resonance harmonic number, and  $\psi$  is here the phase of the Lorentz force acting on electrons with polar coordinates  $R_g$  and  $\psi_g$  of the guiding center radius. For cylindrical waveguides, as shown elsewhere,<sup>23</sup>  $\psi = (s \mp m)\psi_g$  (here  $m$  is the azimuthal index of the operating  $\text{TE}_{m,p}$ -wave). In Eq. (3),  $\theta_0$  is the initial phase at the entrance to the input waveguide which is homogeneously distributed from 0 to  $2\pi$ . Also  $\Delta = (2/\beta_{\perp 0}^2)[(1 - h^2)/(1 - h\beta_{z0})](1 - h\beta_{z0} - s\Omega_0/\omega)$  is the initial mismatch of the cyclotron resonance; the definitions of the normalized wave amplitude  $F$  and beam current parameter  $I_0$  are given in Ref. 23. Note that since below we consider the operation of different stages at different harmonics  $s$ , we use here  $\theta$ ,  $\zeta$ ,  $F$ , and  $I_0$ , which relate to those used previously<sup>10,19,23</sup> (marked by the index ‘‘ $p$ ’’) as  $\theta = \theta_p/s$ ,  $\zeta = \zeta_p/s$ ,  $F = sF_p$ ,  $I_0 = s^2 I_{0,p}$ .

Now let us consider this formalism for each stage of the device in a successive manner.

### A. Input waveguide

As mentioned in the Introduction, the input waveguide can be considered in the frame of the small-signal theory. This means that Eqs. (1)–(3) can be linearized with respect to  $F$ , which yields the known dispersion equation for the propagation constant  $\Gamma$ <sup>22–25</sup>

$$(\Gamma - s\Delta)(\Gamma^2 + I_0 b) - sI_0 \Gamma + sI_0 = 0. \quad (4)$$

As is known,<sup>26</sup> at small  $I_0$  one can introduce  $\gamma = \Gamma/(sI_0)^{1/3}$ ,  $\delta = s\Delta/(sI_0)^{1/3}$ ,  $\zeta' = (sI_0)^{1/3}\zeta$ ,  $w' = w/(sI_0)^{1/3}$ , and  $F' = F e^{is\Delta\zeta}/(sI_0)^{2/3}$ . Then, ignoring small

terms proportional to  $(sI_0)^{1/3} \ll 1$ , one can reduce Eq. (4) to the standard dispersion equation for conventional TWTs with negligibly small space charge effects:<sup>27</sup>

$$\gamma^2(\gamma - \delta) + 1 = 0. \quad (5)$$

This transition from Eq. (4) to Eq. (5) corresponds to reducing Eqs. (1)–(3) to

$$\frac{dw'}{d\zeta'} = -2 \operatorname{Re}\{F' e^{-is\theta_0}\}, \quad (6)$$

$$\frac{d\theta}{d\zeta'} = w', \quad (7)$$

$$\frac{dF'}{d\zeta'} - i\delta F' = -\frac{1}{2\pi} \int_0^{2\pi} e^{is\theta} d\theta_0. \quad (8)$$

Let us point out that Eq. (5) does not contain the cyclotron harmonic number  $s$  directly (although, of course, the normalization parameter  $I_0$  depends on  $s$ , as will be discussed below). Recall that this conclusion has already been reached in the first articles on the theory of cyclotron resonance masers (see, e.g., Ref. 20 and references therein).

Then, as described elsewhere,<sup>19</sup> by solving the dispersion equation [either Eq. (4) or Eq. (5)], one can find the propagation constants for three partial waves and determine the normal wave as superposition of these three. Below we will mostly consider Eq. (5), so the normal wave will be represented as

$$F' = \sum_{l=1}^3 C_l e^{i\gamma_l \zeta'}, \quad (9)$$

where the partial wave amplitudes,  $C_l$ , should be found from the boundary conditions which yield three linear algebraic equations for  $C_l$  (see, e.g., Ref. 19). Substituting this solution for the wave field into Eq. (6) one can determine the normalized energy at the exit from the input waveguide

$$w'(\zeta'_1) = -2 \operatorname{Re} \left\{ e^{-is_1\theta_0} \sum_{l=1}^3 \frac{C_l}{i\gamma_l} (e^{i\gamma_l \zeta'_1} - 1) \right\}. \quad (10)$$

### B. Drift region

In the drift region the electron energy remains unchanged, while the phase varies due to initial energy modulation in the input waveguide. Since there is no wave in the drift region, it makes sense to introduce here a slow variable phase  $\theta_{dr}$ , which will describe the shift of a gyrophase of an initially modulated electron with respect to the gyrophase of an unperturbed electron:  $\theta_{dr} = \Theta - \Theta_{(0)}$ . If we neglect small modulation in the electron axial velocity [which, as follows from comparison of Eqs. (1)–(3) with Eqs. (6)–(8), was already done], the relation between  $\theta_{dr}$  and the phase  $\theta_1$  used in describing the input waveguide operation is simply

$$\theta_{dr} = \theta_1 + \Delta_1 \zeta \quad (11)$$

(here index “1” relates to parameters adopted for the first waveguide). Correspondingly, the equation for the phase  $\theta_{dr}$  has the same form as Eq. (7) with the boundary condition  $\theta_{dr}(0) = \theta_1(\zeta_1) + \Delta_1 \zeta_1$ .

When the drift section is long enough, the ballistic orbital phase bunching in the drift region dominates over phase perturbations in the input waveguide [the latter is determined by the last term in figure brackets in the right-hand side of Eq. (2)]. Correspondingly, the phases  $\theta_1(\zeta_1)$  and  $\theta_{dr}(0)$  can be determined as  $\theta_1(\zeta_1) = \theta_0 - \Delta_1 \zeta_1$  and  $\theta_{dr}(0) = \theta_0$ , respectively, and the phase  $\theta_{dr}$  at the end of the drift region is

$$\theta_{dr}(\zeta'_{dr}) = \theta_0 + w'(\zeta'_1) \zeta'_{dr}.$$

Taking into account Eq. (10), this equation can be rewritten as

$$\theta_{dr}(\zeta'_{dr}) = \theta_0 + q \sin(s_1 \theta_0 - \phi_1). \tag{12}$$

Here we used the representation of the right-hand side of Eq. (10) in the form

$$\sum_{l=1}^3 \frac{C_l}{\gamma_l} [e^{i\gamma_l \zeta'_1} - 1] = |\mathcal{F}_1| e^{i\phi_1}, \tag{13}$$

and introduced the bunching parameter

$$q = 2 |\mathcal{F}_1| \zeta'_{dr}. \tag{14}$$

Note that the amplitudes of partial waves  $C_l$  are linearly proportional to the input wave amplitude  $F'_0$ , since the boundary condition for Eq. (8) is  $F'(0) = \sum_{l=1}^3 C_l = F'_0$ . Therefore we can introduce  $C'_l$  by the relation  $C_l = F'_0 C'_l$ . Correspondingly,  $\sum_{l=1}^3 C'_l = 1$ ,  $|\mathcal{F}_1| = F'_0 |\hat{\mathcal{F}}_1|$ , and  $q = 2 F'_0 |\hat{\mathcal{F}}_1| \zeta'_{dr}$ . As is known (see, e.g., Refs. 27,19), in the absence of electron prebunching at the entrance to the input waveguide the coefficients  $C'_l$  are determined by the following equations:  $\sum_{l=1}^3 C'_l = 1$ ,  $\sum_{l=1}^3 C'_l / \gamma_l = 0$ ,  $\sum_{l=1}^3 C'_l / \gamma_l^2 = 0$ .

### C. Output waveguide

In general, the large-signal operation of the output waveguide can be described by Eqs. (1)–(3) with corresponding cyclotron harmonic number  $s_2$  and boundary conditions. To simplify this treatment we will consider a relatively short output waveguide in the specified current approximation. (The validity of this approximation is checked in the Appendix.) The latter implies that we consider the excitation of the output waveguide by a given current without analyzing the effect of the output waveguide field on electron energies and phases. This simplification reduces the set of Eqs. (1)–(3) to Eq. (3), which in the case of small initial modulation in electron energies and the assumptions just made can be rewritten as

$$\frac{dF_2}{d\zeta} = -I_{02} \frac{1}{2\pi} \int_0^{2\pi} \left\{ \frac{1}{2\pi} \int_0^{2\pi} e^{is_2 \theta(\zeta_{dr}) + i\psi_2} d\theta_0 \right\} d\psi_g. \tag{15}$$

Here an additional averaging over azimuthal coordinates of electron guiding centers appears, which follows from the original averaging of the source term in the wave equation over the interaction cross section. Above, in Eq. (3), this

averaging was eliminated by introducing a properly shifted phase  $\theta$  for each beamlet as discussed after Eq. (3) (see also Ref. 22). So in Eq. (15) for the case of cylindrical waveguides, the exponential term contains the combination of azimuthally dependent terms  $-(s_2/s_1)\psi_1 + \psi_2 = \pm(s_2 m_1 - s_1 m_2)\psi_g/s_1$ . This shows that a beam prebunched by the wave with the azimuthal index  $m_1$  at the cyclotron resonance with the harmonic  $s_1$  will excite at the harmonic  $s_2$  only the wave for which  $s_2 m_1 = s_1 m_2$ , i.e., the wave which is not azimuthally orthogonal to the first one.<sup>28</sup> For such waves the second integration in Eq. (15) is redundant and the integration over  $\theta_0$  determines a corresponding resonant harmonic of the electron current density which, as follows from Eqs. (12) and (15), is equal to

$$j_{s_2} = (-1)^M J_M(s_2 q). \tag{16}$$

Here  $M = s_2/s_1$  is the ratio of the resonant harmonics in two waveguides, i.e., the frequency multiplication factor.

In accordance with Eqs. (15) and (16), the field intensity at the output ( $\zeta = \zeta_2$ ) is equal to

$$|F_2|^2 = I_{02}^2 J_M^2(s_2 q) \zeta_2^2. \tag{17}$$

Note that Eqs. (1) and (3) being properly combined yield the energy conservation law,<sup>22,23,25</sup> which gives the following relation between the so-called orbital efficiency of the device,

$$\eta_{\perp} = \frac{1}{2\pi} \int_0^{2\pi} w(\zeta_2) d\theta_0, \tag{18}$$

and the output field intensity just found,

$$|F_2(\zeta_2)|^2 = I_{02} \eta_{\perp}. \tag{19}$$

(Note that the specified current approximation corresponds to small  $\eta_{\perp}$ .) Also, by relating this intensity to the intensity of the input wave  $|F_0|^2$  excited by a driver at the entrance to the input waveguide, one can determine the gain,

$$G = 20 \log \left\{ I_{02} \zeta_2 \left| \frac{J_M(s_2 q)}{F_0} \right| \right\}. \tag{20}$$

This gain can be represented as  $G_{\text{const}} + G_{\text{var}}$  where the constant part,

$$G_{\text{const}} = 20 \log(I_{02} \zeta_2), \tag{21}$$

is the gain of the output stage (determined in our simplified approximation) and the variable part,

$$G_{\text{var}} = 10 \log \left( \frac{J_M^2(s_2 q)}{|F_0|^2} \right), \tag{22}$$

describes all nonlinear and saturation effects.

In the small-signal regime the Bessel function can be expanded as  $(s_2 q/2)^M/M!$ , which yields the polynomial dependence of the log argument on the intensity of the input wave. Correspondingly, the gain given by Eq. (22) can be represented in the small-signal regime as  $G_{\text{ss}}^{(\text{const})} + G_{\text{ss}}^{(\text{var})}$  where

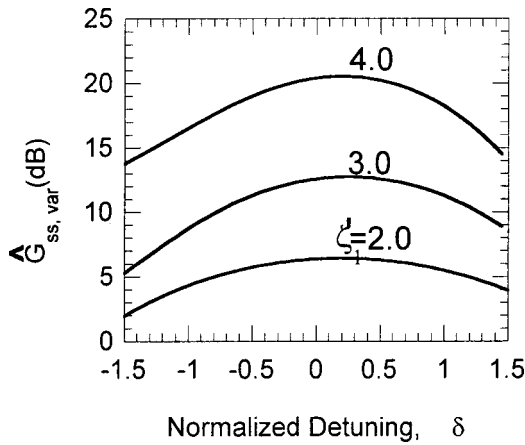


FIG. 1. Variable part of the small-signal gain divided by the frequency multiplication ratio as the function of normalized detuning  $\delta$  for several values of the normalized length of the input waveguide.

$$G_{ss}^{(\text{const})} = 20 \log \left\{ \frac{1}{M!} \left( \frac{s_2 \zeta_{dr}}{(s_1 I_0)^{1/3}} \right)^M |F_0|^{M-1} \right\} \quad (23)$$

and

$$G_{ss}^{(\text{var})} = 20 \log \{ |\hat{\mathcal{F}}_1|^M \}. \quad (24)$$

Here, in Eq. (23) all parameters correspond to notations adopted in Eqs. (1)–(3) and the input wave amplitude  $F_0$ , as shown in Ref. 10, relates to the input power given in kW as

$$F_0 = 0.96 \times 10^{-3} \frac{(1 - h\beta_{z0})^2}{\kappa \gamma_0 \beta_{z0}^3} \sqrt{GP_{in}/h}. \quad (25)$$

Equation (25) is written for the case when the input waveguide operates at the fundamental cyclotron resonance; the coupling coefficient  $G$  for the  $TE_{m,p}$ -wave excited in a circular waveguide is equal to  $J_{m\mp 1}^2(k_{\perp} R_g) / (\nu^2 - m^2) J_m^2(\nu)$ , where  $R_g$  is the guiding center radius of a thin annular electron beam and  $\nu$  is the  $p$ th root of the equation  $J'_m(\nu) = 0$ . Also, in Eq. (25)  $\kappa$  is the transverse wave number,  $k_{\perp}$ , normalized to  $\omega/c$ .

By using Eqs. (5), (13), and (24) one can determine the dependence of the variable part of the small-signal gain on the detuning and normalized length of the input waveguide. Also the saturation effects can be analyzed by studying a simplified version of Eq. (22), namely,

$$G_{\text{var}} = 10 \log \{ J_M^2(s_2 q) \}. \quad (26)$$

Here, in accordance with Eq. (14),  $q = 2|F_0| \zeta'_{dr} |\hat{\mathcal{F}}_1|$ , i.e., this gain as well as the bunching parameter depends on the cyclotron resonance mismatch  $\delta$ .

### III. RESULTS

A small-signal operation of a two-stage frequency-multiplying gyro-TWT is illustrated by Fig. 1, which shows the dependence of the variable part of the small-signal gain on the cyclotron resonance mismatch for several values of the input waveguide length. In accordance with Eq. (24), we plotted in Fig. 1 the value  $\hat{G}_{ss}^{(\text{var})} = G_{ss}^{(\text{var})}/M = 20 \log \{ |\hat{\mathcal{F}}_1| \}$ , which is the same for any frequency multiplication factor. So

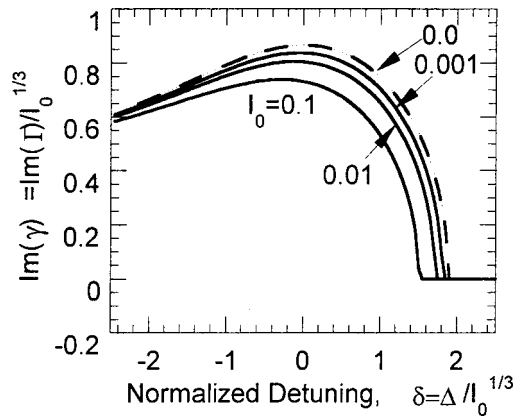


FIG. 2. Growth rate of the wave amplified in the input waveguide as the function of detuning  $\delta$  for several values of the normalized beam current parameter  $I_0$ . The limiting case  $I_0=0$  corresponds to the reducing of the dispersion equation for gyro-TWTs to that for conventional TWTs (in the absence of space charge effects).

the maximum value of the variable part of the gain increases with  $M$ . At the same time, as  $M$  increases, the bandwidth becomes smaller because the gain variation shown in Fig. 1 should be multiplied by  $M$  in order to determine the bandwidth which corresponds to 3 dB deviation in the small-signal gain. For example, in the case of frequency doubling operation to determine the bandwidth one should find from Fig. 1 the range of  $\delta$  corresponding to  $-1.5$  dB degradation; in the case of frequency tripling it should be  $-1$  dB degradation, etc. Note that, although the variable part of the gain, as mentioned above, increases with  $M$ , the total gain does the opposite, since the constant parts of the gain determined by Eqs. (21) and (23) contain the terms which, as  $M$  increases, cause the gain degradation.

In order to evaluate the importance of terms neglected in the process of transition from the dispersion Eq. (4) to its simplified version given by Eq. (5), we also solved Eq. (4) and calculated the corresponding gain. Results are shown in Figs. 2 and 3. In Fig. 2 the growth rate of the growing wave is shown as the function of the normalized cyclotron resonance detuning. The data plotted correspond to solving Eq. (4) with  $s=1$ ,  $b=0$ , and several different values of the beam

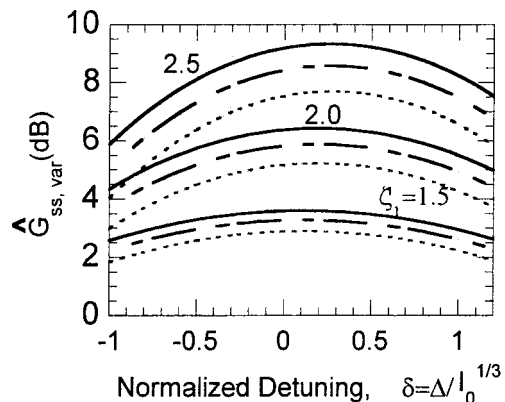


FIG. 3. Variable part of the small-signal gain (the same as shown in Fig. 1) for several values of the normalized beam current parameter  $I_0$ ; solid, dashed, and dotted lines correspond to  $I_0=0, 0.001, \text{ and } 0.01$ , respectively.

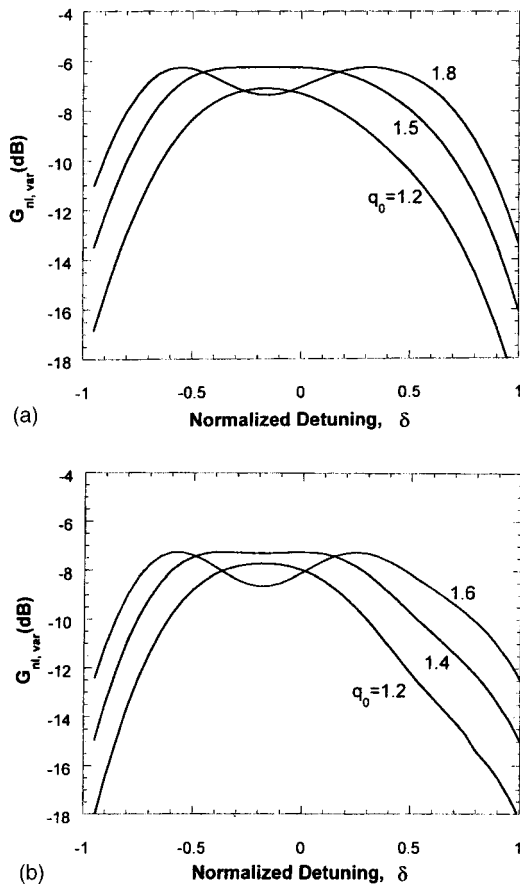


FIG. 4. Variable part of the large-signal gain as the function of normalized detuning  $\delta$  for several values of the bunching parameter  $q_0$  in frequency-doubling (a), and frequency-tripling (b) gyro-TWTs.

current parameter  $I_0$ . The case  $I_0 = 0$  corresponds to Eq. (5). As seen in Fig. 2, the finite values of  $I_0$  cause a certain degradation of the growth rate which is consistent with Ref. 19. The same happens with the small-signal gain shown in Fig. 3. Here solid lines correspond to the TWT-limit [given by the dispersion Eq. (5)], dash-dotted and dotted lines correspond to  $I_0 = 0.001$  and  $0.01$ , respectively.

The saturation effects are illustrated by Fig. 4, which shows the variable gain given by Eq. (26) where the bunching parameter  $q$  is now represented as  $q_0 |\hat{\mathcal{F}}_1(\delta)| / |\hat{\mathcal{F}}_1(0)|$ , i.e.,  $q_0 = 2 |F'_0| |\zeta'_{dr}| |\hat{\mathcal{F}}_1(0)|$  is the bunching parameter in the case of the exact cyclotron resonance. Figures 4(a) and 4(b) correspond to the frequency doubling and frequency tripling regimes, respectively. In the first case ( $M = 2$ ), the maximum variable gain is  $-6.26$  dB and in the second case ( $M = 3$ ) it is  $-7.24$  dB. Note that in the case of standard operation without frequency multiplication ( $M = 1$ ) this gain yields  $-4.7$  dB, so there is no big difference in maximum values of this function  $G_{var}(\delta)$  for different  $M$ .

As seen in Fig. 4, when  $q_0$  exceeds the optimum value,  $q_{opt}$ , which corresponds to the maximum of the variable gain, the valley in the dependence of  $G_{var}$  on  $\delta$  appears at small  $\delta$ . This valley can be explained by the electron overbunching. In such a case the maximum gain corresponds to nonzero detuning which yield  $q_{opt}$ . This formation of two peaks leads to significant bandwidth enlargement. The criti-

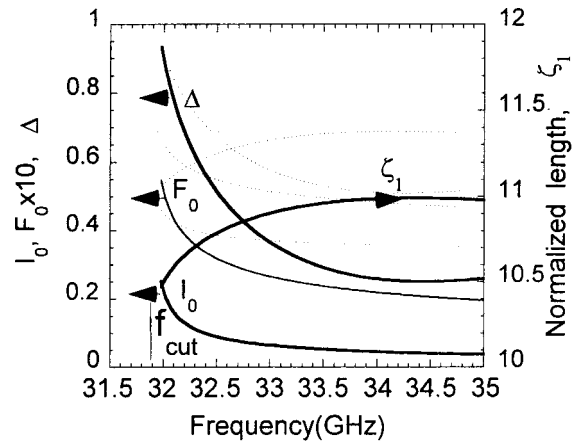


FIG. 5. Frequency dependence of normalized parameters for the experiment described in Ref. 29.

cal value of overbunching corresponds to such  $q_0$  which at zero detuning give the variable gain by 3 dB smaller than in the maximum. These maximum values of  $q_0$  can be found from the analysis of Bessel functions: for frequency-doubling devices  $q_{opt} = 1.527$  and  $q_{0,max} = 2.038$ , and for frequency-tripling devices  $q_{opt} \approx 1.4$  and  $q_{0,max} \approx 1.761$ .

#### IV. DISCUSSION

In the analysis done above, we studied the gain assuming some normalized parameters to be fixed. In real experiments practically all these parameters depend on the operating frequency. Therefore, to accurately analyze the bandwidth this frequency dependence should be taken into account.

As an example, let us consider parameters of a severed gyro-TWT described in Ref. 29, assuming that for frequency doubling operation the sever is followed by an output waveguide operating in the  $TE_{21}$ -mode (an input waveguide operates in the  $TE_{11}$ -mode at the fundamental resonance). The tube described in Ref. 29 was driven by a 90 kV, 2A electron beam with an orbital-to-axial velocity ratio close to 1.0 and the guiding center radius  $R_g = 0.33R_w$ . The waveguide radius,  $R_w$ , was equal to 0.2757 cm, the length of the input waveguide was 8.25 cm, and the length of the separation was 3 cm. The driver produced up to 1 kW power and the drive frequency was varied from 32 to 36 GHz.

For this tube the dependence of normalized parameters used above on the drive frequency is shown in Fig. 5 (here the cyclotron resonance mismatch  $\Delta$  is shown for the magnetic field equal to 12.15 kG). Note that for a given waveguide the cutoff frequency of the  $TE_{1,1}$ -wave is equal to 31.886 GHz (shown in Fig. 5). Also recall that, when the drive frequency approaches the cutoff, our formalism should be modified since we neglected the electron interaction with a nonsynchronous backward wave while near cutoff this interaction must be taken into account.

Among the dependencies shown in Fig. 5, at first glance, the most surprising is the frequency dependence of the cyclotron resonance mismatch  $\Delta$ . This dependence shows that in a certain range of frequencies the mismatch  $\Delta$  remains practically unchanged. To explain this one should bear in

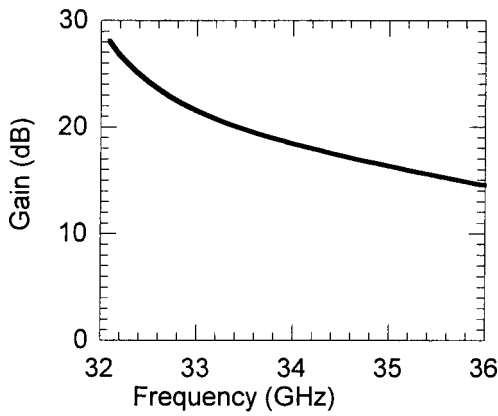


FIG. 6. Gain vs frequency for the experiment (Ref. 29).

mind that the mismatch  $\Delta$  contains the frequency dependent Doppler term  $k_z v_z$ , i.e.,  $\Delta \sim 1 - h\beta_{z0} - s\Omega_0/\omega$ . By differentiating this mismatch one can easily find that the changes in frequency do not affect the mismatch  $\Delta$  when the device operates at the grazing condition  $v_{gr} = v_{z0}$ . Here  $v_{gr} = d\omega/dk_z$  is the group velocity of the wave. In the case of  $\Delta$  shown in Fig. 5 for  $B_0 = 12.15$  kG,  $d\Delta/df = 0$  corresponds to  $f \approx 34.45$  GHz.

The corresponding dependence of the gain on the drive frequency is shown in Fig. 6. As follows from Fig. 6, with the departure from cutoff the gain decreases while the bandwidth increases. A relatively small value of the gain can be

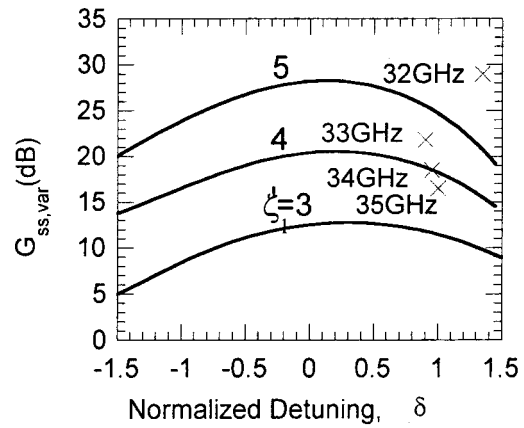


FIG. 7. General dependencies of the variable part of the small-signal gain on the normalized frequency detuning and the data corresponding to the experiment (Ref. 29) for several frequencies.

explained by the use of a specified current approximation for the short output waveguide. A more accurate analysis of an extended output waveguide, certainly, would allow us to increase the gain. For illustrative purposes, in Fig. 7 there are also shown the data corresponding to this experiment in the same plot as a previously calculated small-signal gain. The fact that the changes in the drive frequency do not change significantly the normalized detuning can be explained, first, by the discussed-above nonlinear dependence of the detuning  $\Delta$  on the signal frequency and, second, it can be explained by

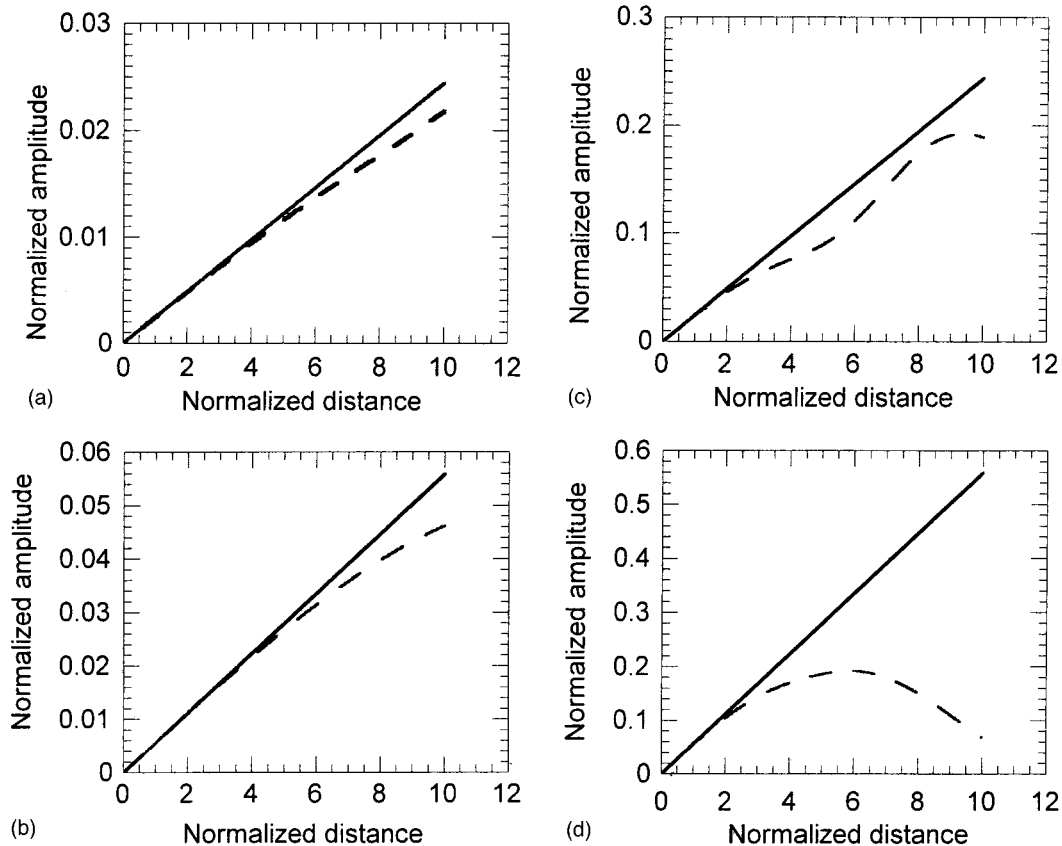


FIG. 8. Wave amplitude as the function of the axial coordinate calculated in the specified current approximation (solid curves) and by using a self-consistent set of equations (dashed curves): (a)  $I_{02} = 0.01$ ,  $q = 0.5$ , (b)  $I_{02} = 0.01$ ,  $q = 1.5$ , (c)  $I_{02} = 0.1$ ,  $q = 0.5$ , and (d)  $I_{02} = 0.1$ ,  $q = 1.5$ .

the frequency dependence of the normalized beam current parameter  $I_0$  to which the detuning  $\delta$  is normalized.

This example shows that for correct evaluation of the bandwidth in real devices it is not enough to use general dependencies of the gain on the normalized detuning (similar to those shown in Figs. 1, 3, and 4). We should also be concerned about the dependencies of normalized parameters on the operating frequency.

## V. SUMMARY

In this article, we presented the analytical theory describing the gain and bandwidth of frequency-multiplying gyro-TWTs. The analysis of frequency-doubling and frequency-tripling gyro-TWTs has been carried out. Also shown was how to use the developed theory for evaluating the operating characteristics of real devices.

## ACKNOWLEDGMENTS

This work has been supported by the Multidisciplinary University Research Initiative on Vacuum Electronics sponsored by the Air Force Office of Scientific Research (AFOSR) and by the Naval Research Laboratory.

## APPENDIX: VALIDITY OF A SPECIFIED-CURRENT APPROXIMATION

To check the validity of the specified-current approximation we did simulations for the output waveguide described by Eqs. (1)–(3) with the boundary condition for the phase given by Eq. (12) and compared these results with those based on the use of Eq. (15). The results are shown in Fig. 8 where the axial dependence of the wave amplitude is shown for several values of the normalized beam current  $I_0$  and the bunching parameter [the cyclotron resonance mismatch  $\Delta$  present in Eq. (2) is taken equal zero]. The results shown indicate that at small values of the parameter  $I_0$  [ $I_0=0.01$ , see Figs. 8(a) and 8(b)], the specified current approximation works well up to the normalized length of the output waveguide of about  $\zeta_2=4$ . In the case of large values of  $I_0$  [ $I_0=0.1$ , see Figs. 8(c) and 8(d)] the region of validity of this approximation is restricted by  $\zeta_2 \leq 2$ . Note that for parameters of the experiment<sup>29</sup> discussed above, these normalized lengths correspond to  $L_2/\lambda_2 \approx 6.8$  and 3.4, respectively.

- <sup>1</sup>K. L. Felch, B. G. Danly, H. R. Jory, K. E. Kreischer, W. Lawson, B. Levush, and R. J. Temkin, Proc. IEEE **87**, 752 (1999).
- <sup>2</sup>E. V. Zasyplin, M. A. Moiseev, I. G. Gachev, and I. I. Antakov, IEEE Trans. Plasma Sci. **24**, 666 (1996).
- <sup>3</sup>Q. C. Wang, D. B. McDermott, and N. C. Luhmann, Jr., IEEE Trans. Plasma Sci. **24**, 700 (1996).
- <sup>4</sup>W. Lawson, H. W. Matthews, J. P. Calame, M. K. E. Lee, J. Cheng, B. Hogan, P. E. Latham, V. L. Granatstein, and M. Reiser, Phys. Rev. Lett. **71**, 456 (1993).
- <sup>5</sup>W. Lawson, P. E. Latham, J. P. Calame, J. Cheng, B. Hogan, G. S. Nusinovich, V. Irwin, V. L. Granatstein, and M. Reiser, J. Appl. Phys. **78**, 550 (1995).
- <sup>6</sup>H. Guo, S. H. Chen, V. L. Granatstein, J. Rodgers, G. Nusinovich, M. Walter, B. Levush, and W. J. Chen, Phys. Rev. Lett. **79**, 515 (1997).
- <sup>7</sup>G. S. Nusinovich and O. Dumbrajs, Phys. Plasmas **2**, 568 (1995).
- <sup>8</sup>G. S. Nusinovich, B. Levush, and O. Dumbrajs, Phys. Plasmas **3**, 3133 (1996).
- <sup>9</sup>G. S. Nusinovich, G. P. Saraph, and V. L. Granatstein, Phys. Rev. Lett. **78**, 1815 (1997).
- <sup>10</sup>G. S. Nusinovich and M. Walter, Phys. Plasmas **4**, 3394 (1997).
- <sup>11</sup>K. R. Chu, H. Guo, and V. L. Granatstein, Phys. Rev. Lett. **78**, 4661 (1997).
- <sup>12</sup>J. L. Seftor, V. L. Granatstein, K. R. Chu, P. Sprangle, and M. Read, IEEE J. Quantum Electron. **15**, 848 (1979).
- <sup>13</sup>L. R. Barnett, Y. Y. Lau, K. R. Chu, and V. L. Granatstein, IEEE Trans. Electron Devices **28**, 872 (1981).
- <sup>14</sup>G. S. Park, J. J. Choi, S. Y. Park, C. M. Armstrong, A. K. Ganguly, R. H. Kyser, and R. K. Parker, Phys. Rev. Lett. **74**, 2399 (1995).
- <sup>15</sup>M. A. Moiseev, Radiophys. Quantum Electron. **20**, 846 (1977).
- <sup>16</sup>A. K. Ganguly and S. Ahn, IEEE Trans. Electron Devices **31**, 474 (1984).
- <sup>17</sup>K. R. Chu, H.-Y. Chen, C.-L. Hung, T.-H. Chang, L. R. Barnett, S.-H. Chen, T.-T. Yang, and D. J. Dailitis, IEEE Trans. Plasma Sci. **27**, 391 (1999).
- <sup>18</sup>K. T. Nguyen, J. P. Calame, D. E. Pershing, B. G. Danly, M. Garven, B. Levush, and T. Antonsen, Jr., "Design of a Ka-Band Gyro-TWT for Radar Applications," IEEE Trans. Electron Devices (to be published).
- <sup>19</sup>G. S. Nusinovich and M. Walter, Phys. Rev. E **60**, 4811 (1999).
- <sup>20</sup>A. V. Gaponov, M. I. Petelin, and V. K. Yulpatov, Radiophys. Quantum Electron. **10**, 794 (1967).
- <sup>21</sup>A. I. Denisov, Radiotekh. Elektron. (Moscow) **6**, 212 (1961).
- <sup>22</sup>A. W. Fliflet, Int. J. Electron. **61**, 1049 (1986).
- <sup>23</sup>G. S. Nusinovich and H. Li, Int. J. Electron. **72**, 895 (1992).
- <sup>24</sup>A. V. Gaponov, Izv. Vyssh. Uchebn. Zaved., Radiofiz. **4**, 547 (1961).
- <sup>25</sup>N. S. Ginzburg, I. G. Zarnitsyna, and G. S. Nusinovich, Radiophys. Quantum Electron. **24**, 331 (1981).
- <sup>26</sup>V. K. Yulpatov, Radiophys. Quantum Electron. **10**, 471 (1967).
- <sup>27</sup>J. R. Pierce, *Traveling Wave Tubes* (Van Nostrand, Princeton, 1950).
- <sup>28</sup>M. A. Moiseev and G. S. Nusinovich, Radiophys. Quantum Electron. **17**, 1305 (1974).
- <sup>29</sup>K. R. Chu, L. R. Barnett, W. K. Lau, L. H. Chang, and C. S. Kou, *IEDM Technical Digest*, International Electron Devices Meeting, San Francisco, 9–12 December 1990 (IEEE, Piscataway, NJ, 1990), p. 699.